Secernin-1 is a Novel Protein Involved in Alzheimer's Disease

Neural Science Honors Thesis

By

SACHA KER MCELLIGOTT

Supervisor:
THOMAS WISNIEWSKI, MD

NEW YORK UNIVERSITY
DECEMBER 2018

Abstract

Amyloid plaques and neurofibrillary tangles (NFTs) are the two pathological hallmarks that define Alzheimer's disease (AD). Recently, our team completed the most comprehensive analysis of the plaque proteome to date, and revealed a variety of novel proteins which had never before been implicated in the disease. Among these, Secernin-1 (SCRN1) exhibited consistently high expression in amyloid plaques. SCRN1 has been primarily identified as a cytosolic protein that regulates mast cells. Previous studies have also suggested that misregulation of SCRN1 may have a contributing role in a variety of cancers, as well as schizophrenia and bipolar disorder. However, very few studies have associated SCRN1 with AD, and a definitive role of SCRN1 in AD pathology remains elusive.

Here, I used fluorescent immunohistochemistry on sections of various regions from formalin-fixed paraffin-embedded, AD brain tissue, to show that SCRN1 colocalizes with phosphorylated Tau (pTau), present in both NFTs and dystrophic neurites. I compared these results to identically treated tissue from non-demented controls, which showed ubiquitous, yet low, levels of SCRN1. Surprisingly, SCRN1 staining also demonstrated variation across brain regions and across individuals, suggesting a possible occurrence of SCRN1 distribution in AD pathology.

More recent efforts have further characterized patterning between SCRN1 and different pTau antibodies, each of which has selective affinity for various residues of pTau. My results show that SCRN1 consistently colocalized with PHF1—which is a monoclonal antibody that targets specific pTau serine residues, in NFTs. Subsequent analysis revealed significant correlations between the expressions of PHF1 and SCRN1 inside PHF1-positive neurons across three brain regions for both early and late-stage AD patients. In addition, the success of machine learning classification to label brain tissue using SCRN1 staining has reinforced the strong association between SCRN1 and AD.

Overall, the preliminary data generated from this study imply a potential relationship between SCRN1, pTau and cognitive impairment.

TABLE OF CONTENTS

CHAPTER 1

INTRODUCTION

First described by Dr. Alois Alzheimer in 1906, Alzheimer's disease (AD) is one of the leading causes of death and is the most common form of dementia (alz.org). Recent estimates state that 5.4 million individuals are afflicted with it, and that it may in fact be the third leading cause of death (alz.org) (nih.gov). Experts predict that by 2050—the year my generation will be of age for early onset AD—the number of people living with the disease will be 13.8 million (alz.org). Despite decades of effort, current treatments offer little symptomatic relief, and a definitive cause for the disease remains elusive. Yet, due to their abundance in post-mortem analysis of AD brain tissue, amyloid plaques and neurofibrillary tangles (NFTs) are the two structures currently used to pathologically define AD.

Aβ has long been considered a crucial hallmark in AD development. Decades of research have supported the claim that inadequate Aβ clearance—and thus the accrual of extracellular Aβ deposits—is among the earliest factors in AD pathology (Selkoe and Hardy, 2016; Wang et al., 2017). The hyperphosphorylation of tau proteins, which are chiefly responsible for the structural integrity of neural cells, leads to the development of

the intraneuronal inclusions, NFTs. The abundance of both hallmarks leads to excitotoxicity and neuronal death. Specifically, the presence of NFTs prevents adequate nutrient passage in affected neurons which eventually leads to cell death. In addition to their abundance in neurons, NFT-like structures have been shown to be found in glial cells in AD patients, thus positioning NFTs as the most pervasive hallmark in AD (Ikeda et al., 1998). Due to the prevalence of these structures, and the importance of finding drug targets, perhaps the greatest investment in the field of AD research has been trying to understand the composition and architecture of these pathological hallmarks.

The findings from past proteomic studies have furthered our understanding of the plaque proteome, revealing a variety of novel proteins never before implicated in AD (Drummond et al., 2018; Ping et al., 2018). In addition, novel biomarkers have been found using the proteomic approach on blood plasma in elder patients (Guo et al., 2013). In our lab, we used a proteomic approach to uncover the hidden proteins inside of AD hallmarks. Specifically, by isolating Aβ plaques, from human brain tissue using a laser microscope and analyzing the composition of these plaques using liquid chromatography-mass spectrometry, the team and I were able to determine a richer portrait of the protein composition of plaques than had any previous studies (Drummond et al., 2017).

Among these proteins, our team showed that Secernin-1 (SCRN1) exhibited consistently high expression in amyloid plaques. SCRN1 has been primarily identified as a cytosolic protein that regulates exocytosis in mast cells (Way et al., 2002). Previous studies have also suggested that misregulation of SCRN1 may have a contributing role in a variety of cancers, as well as schizophrenia and bipolar disorder. Additionally, past research has demonstrated the abundance of insoluble SCRN1 among total insoluble aggregates in human Alzheimer's brain homogenates, as well as in immuno-purified aggregates from tau and Aβ (Ayyadevara et al., 2016). However, despite such evidence, literature linking SCRN1 and AD are sparse, and a definitive role for this protein in AD

pathology remains unknown.

Using fluorescent immunohistochemistry on sections of various regions from formalin-fixed paraffin-embedded, early onset and late-stage AD brain tissue, I showed that SCRN1 colocalizes with phosphorylated Tau (pTau), present in both NFTs and dystrophic neurites. I compared these results to identically treated tissue from non-demented controls. Additionally, analysis of the fluorescent stainings reveals a significant correlation between the expressions of SCRN1 and pTau in frontal cortex and hippocampus for AD and early AD tissues. Such findings implicate SCRN1 as a novel protein involved in AD, and thus warrant further investigation into the specific mechanisms by which it contributes to AD pathology. However, before targeting SCRN1 as a potential drug target, it is crucial to first confirm that its expression in AD is notably different than that in normal controls (NC).

To assess the predictive power of SCRN1 for classifying the pathology of brain tissue, I developed a computational model that could distinguish between AD and NC samples, using a machine learning classifier trained solely on fluorescent images of SCRN1 in different brain regions. This model thus offers a framework for assessing the specific features of its expression that make AD distinguishable from NC, and perhaps implicate certain mechanisms by which SCRN1 drives AD pathology. My classifier successfully identifies the pathology of patients using small regions of interest (containing about 250 neurons each) in entorhinal cortex, temporal cortex, and the CA regions of the hippocampus—the success of this model offers the first, conclusive evidence for the predictive power of SCRN1 in the context of AD.

While the exact mechanisms of involvement for SCRN1 in AD still warrant further investigation, these results are the first to conclusively demonstrate that SCRN1 is involved in AD for all stages of the disease. Furthermore, these results show that SCRN1 is involved in both of the primary pathological hallmarks of AD, thus catapulting SCRN1

into the spotlight as a novel candidate for contributing to AD development. In all, the findings from my research open the door to a promising alternative to conventional studies of AD—after over a century of research and innumerable initiatives to tackle AD, perhaps SCRN1 is the answer for which we have been looking.

CHAPTER 2

METHODS

2.1 Immunohistochemistry

In order to characterize the expression patterns of our proteins of interest, I began my analysis using fluorescent immunohistochemistry (IHC) on formalin-fixed, paraffin-embedded, AD and NC human brain tissue. Consent protocol for these tissue samples was completed in accordance with the internal review board of NYU Langone Medical Center. For further confidence in the tissue, the AD pathology of each brain was confirmed by a certified neuropathologist. Each tissue was cut and placed onto either a PEN membrane FrameSlide (Leica Biosystems, cat#LCM0522) or a Snowcoat Clipped Corner Slide (Leica Biosystems, cat# unknown). To deparaffinize tissue while limiting damage to the integrity of the sample, I submerged each sample in a glass container of xylene for a total of 10 minutes, subsequently submerging the tissue in increasing concentrations of ethanol solutions, for 5 minutes each. In order to break any protein cross-links resulting from the formalin treatment of the tissue, I exposed samples to 7 minutes of formic acid, after which the samples were rinsed with phosphate-buffered saline (PBS). To further the

breakage of cross-links, and thus minimize blockage between antigens and antibodies, samples were then treated with a citrate buffer and heated, then blocked with normal goat serum (MP Biomedicals, cat#0864292), per standard IHC protocols. After blocking, the tissues were exposed to primary antibodies.

All antibodies were administered in concentrations optimized for adequate visualization of proteins with minimal antibody expenditure. To visualize the protein expression in my samples I used the following primary antibodies: 1:200 dilution in Phosphate Buffered Saline Tween-20 (PBST) of anti-PHF1, an in-house antibody established to recognize and bind to specific serine residues of pTau, 4G8 anti-Aβ (BioLegend, cat#SIG-39220), and an industry-standard anti-SCRN1 mouse antibody (LifeSpan Biosciences, cat#LS-C324947) at 1:100 dilution in PBST (Otvos et al., 1994).

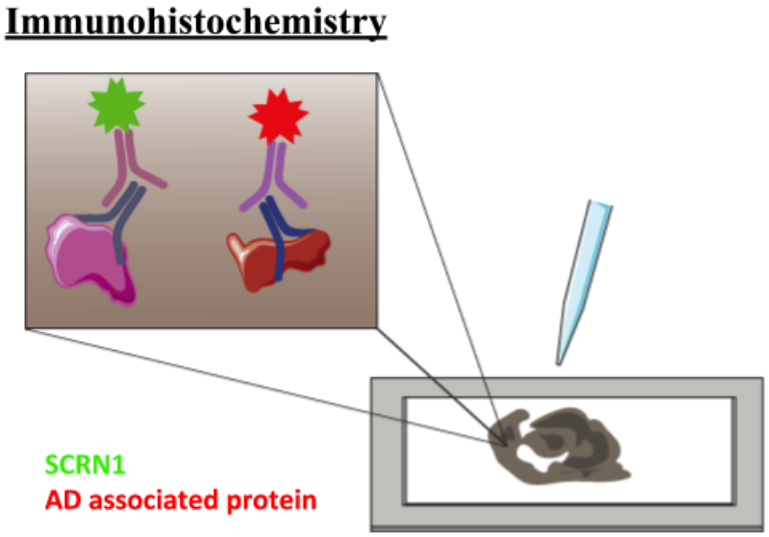

FIGURE 2.1. **Schematic representation of IHC approach**
Brain slices from late-stage AD patients were stained for SCRN1 and a pathological hallmark using IHC. The protein of interest is bound by primary antibodies, which are bound by secondary antibodies chemically conjugated to fluorescent chromophores. This process allows for the visualization of protein expression in tissue

It is important to note that my selection of pathological hallmark to visualize changed with each experimental goal, however, the rest of the protocol remained the same. The

brain tissues were incubated overnight in the primary antibody solutions, so as to ensure sufficient interaction with target proteins. After the overnight incubation with primary antibodies, samples were then exposed for 2 hours to the secondary antibodies, which included: 488-conjugated rabbit immunoglobulin G (IgG) (Jackson ImmunoResearch, cat#111-545-144) and 647-conjugated mouse IgG (Jackson ImmunoResearch, cat#115-605-164), with a 1:500 dilution in PBS for both. Both the timing of exposure and the concentration of antibody were tested and confirmed prior to experimentation. After incubation with secondary antibodies, the samples were rinsed with saline solution and exposed for 10 minutes in a Hoechst solution for eventual visualization of cell nuclei. Finally, slides were coverslipped and stored in a dark containment unit to dry.

2.2 Isolation of Plaques and Analysis of Proteome

In order to conduct localized proteomics on the Aβ plaques, I first needed to visualize their expression. To do this, I stained for Aβ using the aforementioned protocol. I then loaded each stained slide into a LMD6500 microscope (Leica Biosystems, ca#11501478), with which I could precisely isolate stained structures using laser capture microdissection (LCM). In order to collect the isolated plaques after LCM, I placed a collection tube (Leica Biosystems, cat# unknown) underneath the slides and guided the laser to cut around the perimeter of the plaques. Due to the gravitational force on the tissue, collection of isolated plaques was consistent, and the efficacy of this process was subsequently confirmed by visualizing the contents of the collection cap. The lab and I conducted this process on brain tissue from 22 patients with late-stage AD, collecting roughly 2mm^2 of plaques from the hippocampus per brain. This protocol is detailed further in past publications from the lab (Drummond et al., 2017; Drummond et al., 2015).

The average protein composition of the collected plaques were determined by liquid chromatography-mass spectrometry (LC-MS), which was conducted by the NYU Langone

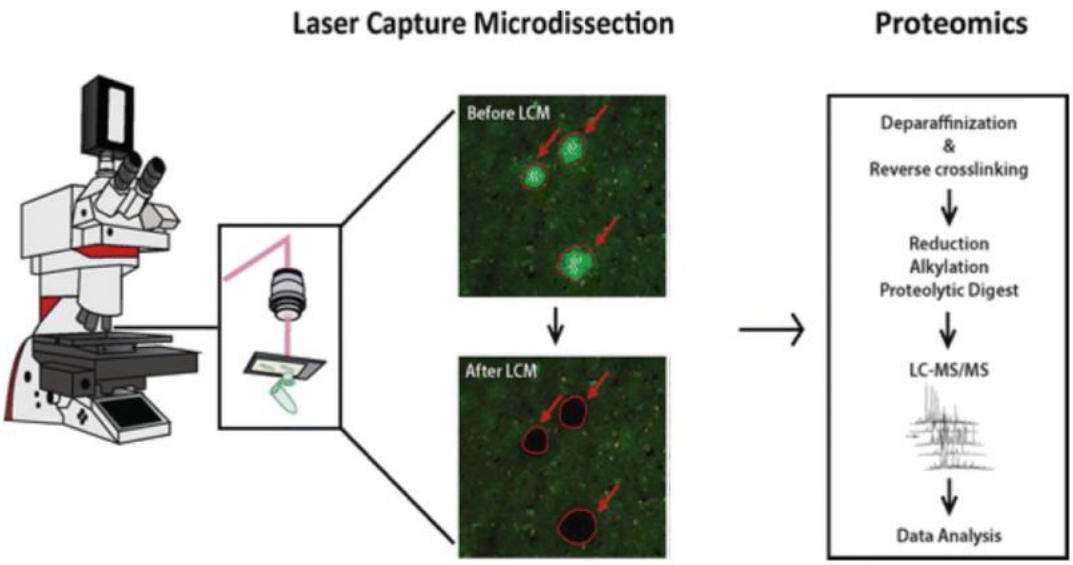

FIGURE 2.2. **Schematic representation of localized proteomics**
Plaques from human late-stage AD brain tissue were stained using IHC and isolated using LCM. Plaques were collected from each subject and the protein composition was analyzed using LC-MS. Figure modified from Drummond et al., 2018

Proteomic Laboratory using established protocols from previous studies (Drummond et al., 2015). Finally, the proteomic results of the LC-MS were loaded into an Excel file and uploaded to a local server, from which I could access them.

2.3 Data Analysis

Scans of the stained slides were generated using an auto-scanner in the NYU Langone Department of Cell Biology and uploaded to an online server. Smaller images were then saved onto a computer using screen captures of the regions of interest (ROIs) from each scan. The ROIs for each brain region were determined *a priori* in accordance with

previous neuropathological tangle data in AD (Drummond et al., 2015).

To quantify the fluorescence of SCRN1 and PHF1 in ROIs, I loaded the images into ImageJ (National Institutes of Health), and developed macro scripts to extract the desired data. The algorithm I developed is as follows: first, the images were isolated into their red-green-blue (RGB) constituent values, each channel representing a different stain (red: PHF1, green: SCRN1, blue: Hoechst). Using the images from the red channel, a threshold for PHF1 intensity and object size was used to identify and isolate tangles from the ROIs, and the resulting intensities of each identified object were loaded into an array on Google Sheets. The mask of the identified objects was then superimposed on the green channel, and used to calculate the SCRN1 intensities in each object. These data were loaded into an adjacent column of the aforementioned array, and linear regressions were generated using a built-in toolbox in Google Sheets. To calculate the significance of the correlations, I then compared the calculated *Pearson's r* with the sample size for the given dataset using statistical toolboxes in the programming language, R.

All other figures and resulting analyses were generated using either Google Sheets, MATLAB (Mathworks), R, or Python, along with the associated toolboxes.

Despite having a generous number of patients with AD represented in my sample pool, the scans yielded insufficient data to train a neural network from scratch. To address this, I used an open-source retraining pipeline in TensorFlow (Google) to develop my machine learning classifier. Specifically, I exploited the scalable architecture of the convolutional neural network model, Inception v3, to develop a classifier that did not require a massive dataset on which to train (Szegedy et al., 2015). Since one of the main pillars of Inception v3 is reducing representational bottlenecks, the model limits dimensionality reduction, which makes retraining on a small number of images that share certain feature dimensions tractable. In order to create invariance for irrelevant features of the images, I created 3 versions of each ROI image, saving copies of each

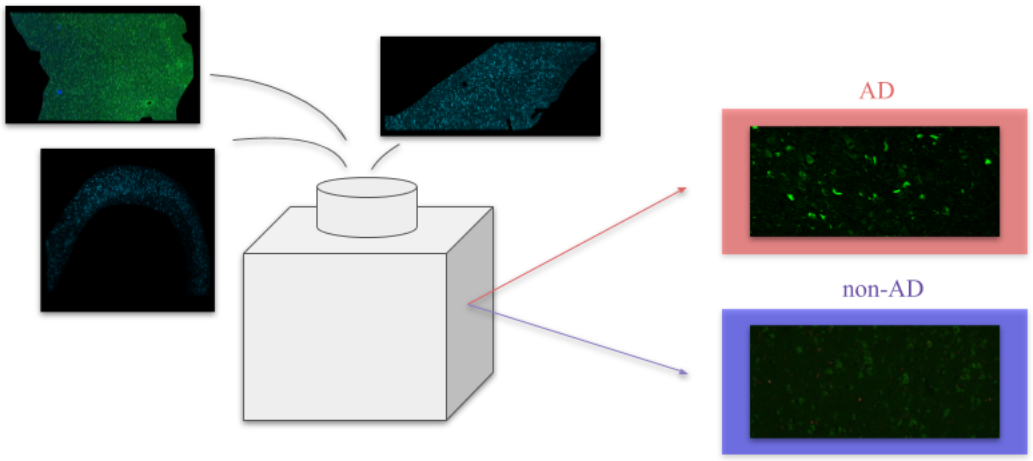

FIGURE 2.3. **Schematic representation of ML classification**
A convolutional neural network trained for classification of flowers was retrained on images of SCRN1-stained ROIs in AD and NC brains, and tested on its ability to identify the pathology of an ROI based on the expression of SCRN1. Images were fed into the model and predictive features of SCRN1 expression were extracted by the model, from which it would generate predictions as to the pathology

image that were flipped horizontally, vertically, and both. The classifier was retrained on 1,068 images (taken from 18 AD patients and 18 NC) of SCRN1 stained ROIs. The efficacy of this classifier was then tested on a reserved test set of 100, randomly selected images (50 AD, 50 NC) from the training set, using a binary classification paradigm, labelling each image independently.

CHAPTER 3

RESULTS

3.1 SCRN1 colocalizes with the pathological hallmarks of AD

3.1.1 SCRN1 and Aβ Plaques

In order to determine whether SCRN1 is involved in AD, I needed to first confirm that SCRN1 was indeed found inside of the pathological hallmarks most closely associated with the disease. Using the IHC staining method outlined in Methods, I stained for SCRN1 and Aβ plaques in the hippocampus of 5 late-stage AD patients.

The results of these stainings revealed a colocalization pattern that dominated in cortical areas hugging the perimeter of the hippocampus. However, the regions directly surrounding the hippocampus also showed a consistent colocalization pattern, though SCRN1 was found to be less abundant and the patterning was notably different. For example, whilst the cortical plaques exhibited a pattern of high SCRN1 throughout the plaque, SCRN1 inside the hippocampal plaques formed punctae that appeared to be enveloped by the Aβ staining. These results corroborated my findings from the proteomic

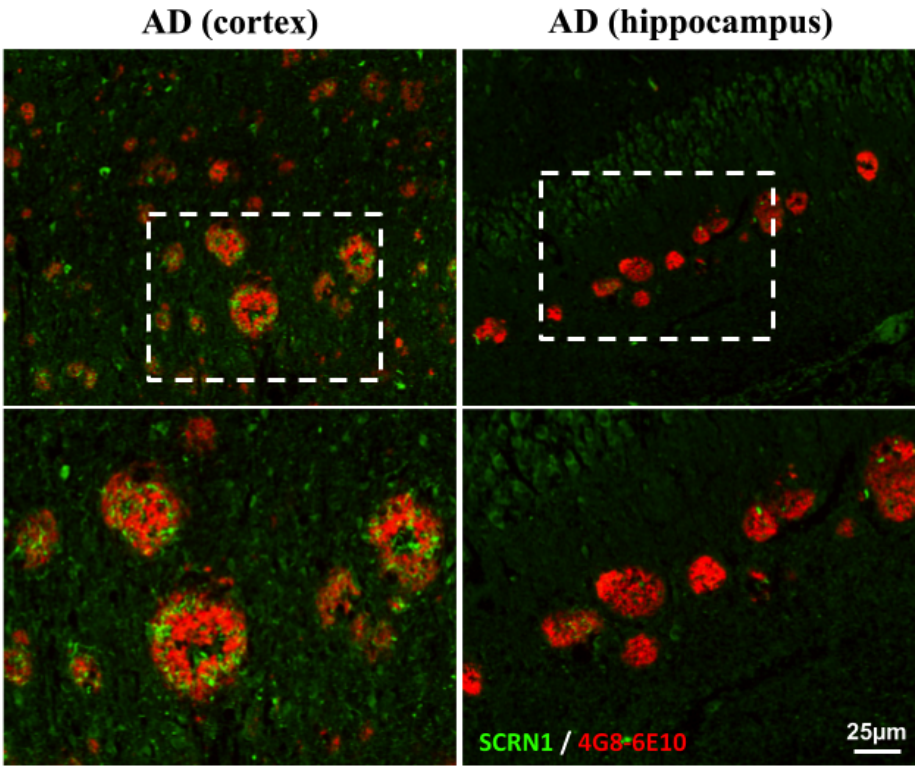

FIGURE 3.1. **Aβ and SCRN1**
Typical colocalization patterns of Aβ and SCRN1 in the two regions, shown from a late-stage AD patient. These fluorescent images were contrast adjusted to dampen background noise

analysis and strengthen the potential for a relationship between SCRN1 and AD.

3.1.2 SCRN1 and NFTs

While the colocalization between SCRN1 and Aβ was apparent, I wanted to understand the expression patterns of SCRN1 relative to NFTs, and thus I stained for SCRN1 and PHF1 in slices of the hippocampus, temporal cortex (TCx), and entorhinal cortex (ECx) in NC, early-onset AD, and late-stage AD brains. In addition, I stained for SCRN1 and PHF1 in the frontal cortex and midbrain of NC and AD brains. NC tissues showed uniform and ubiquitous intraneuronal SCRN1 staining, with very little PHF1 staining, across all three brain regions.

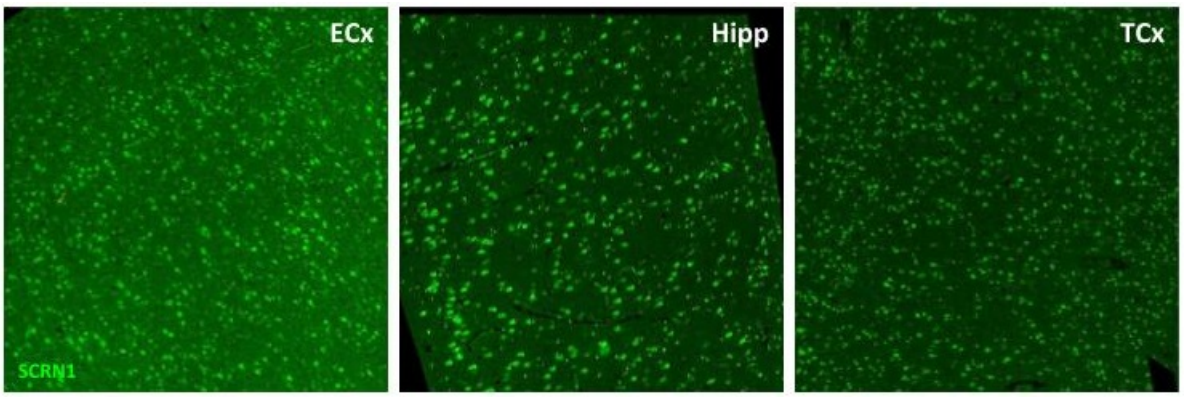

FIGURE 3.2. **SCRN1 in controls**
Representative SCRN1 staining of NC patients in the three regions (images normalized)

While the SCRN1 expression across neurons appeared uniform in the NC samples, the neurons in early-onset AD and late-stage AD samples showed progressively wider distributions of SCRN1 intensities. This result was consistent across the three brain regions studied. While the SCRN1 intensity distribution was notably wider as a function of disease progression, the total pixel count remained comparable, with total, average, non-zero, hippocampal pixel counts of 6.9504e+05, 7.4026e+05, and 6.0919e+05 for AD, early AD, and NC respectively.

In addition to the widening distribution, a strong, intraneuronal colocalization pattern between SCRN1 and PHF1 was found in all studied regions in early AD and late-stage AD brains. The ubiquity of this pattern only slightly varied across subjects with the same pathology.

3.2 The expressions of SCRN1 and PHF1 are correlated across brain regions and stages of AD

I conducted regression analysis of SCRN1 and PHF1 intensities inside of neurons across the two pathologies in the hippocampus, TCx, and ECx. To do this, I identified PHF1-

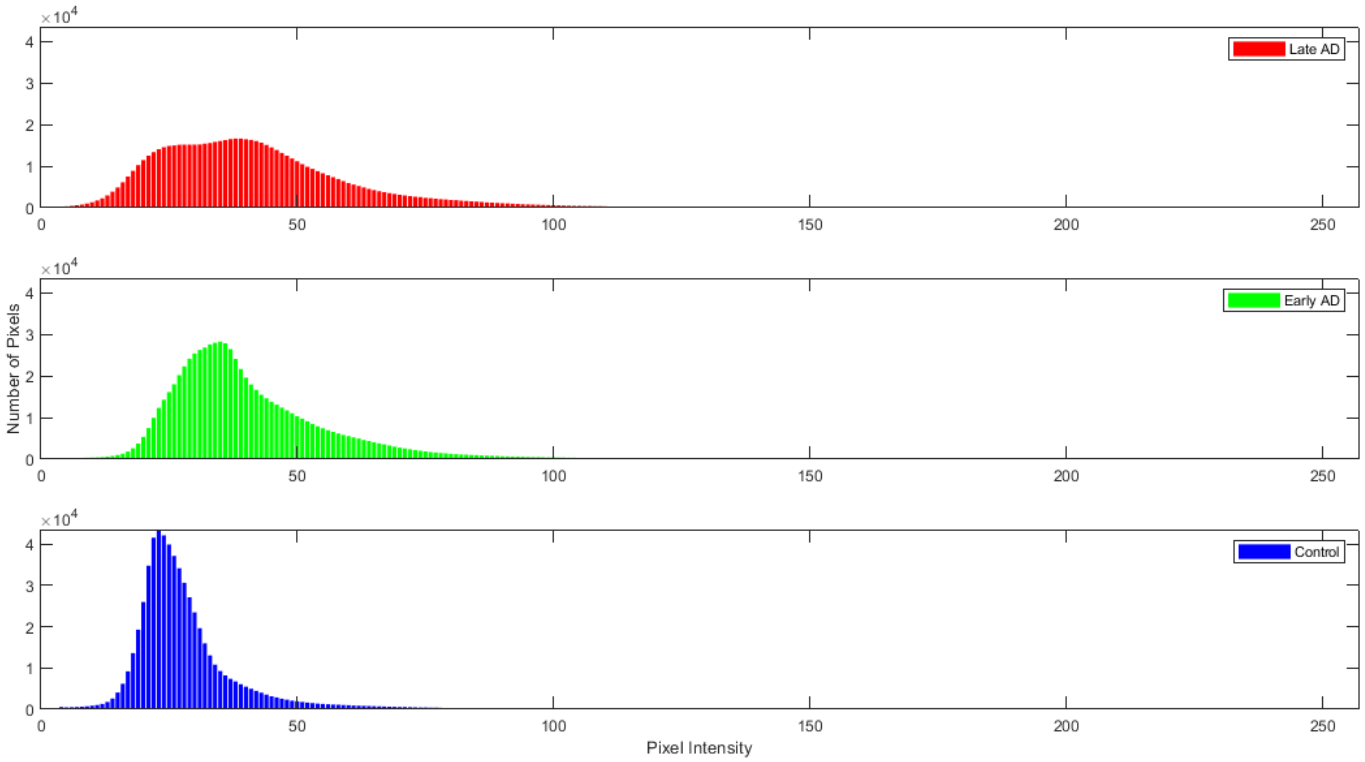

FIGURE 3.3. **SCRN1 intensity distribution across pathologies**
Average intensity histograms for SCRN1 stained ROIs in the hippocampus across patients (7 AD, 11 early AD, 10 NC)

positive neurons based on the intensity of PHF1 as well as the size and shape of the objects in each ROI, and generated linear regressions on cumulative SCRN1 and PHF1 intensity data from all the patients (AD = 18, early AD = 11) for each region and pathology. Consistent with the neuropathological classification of the brain tissue, NC samples lacked sufficient PHF1-positive objects to conduct this analysis. For a closer look at the specifics of the remaining analyses, please refer to Methods.

The results of the regression analysis reveal a significant, positive correlation between the intensities of SCRN1 and PHF1 in neuron-labelled objects in early onset AD and late-stage AD brains ($p < .00001$ for all regressions, *Pearson's r* critical value distribution, one-tailed). The correlations for all regions in early AD were higher than those for

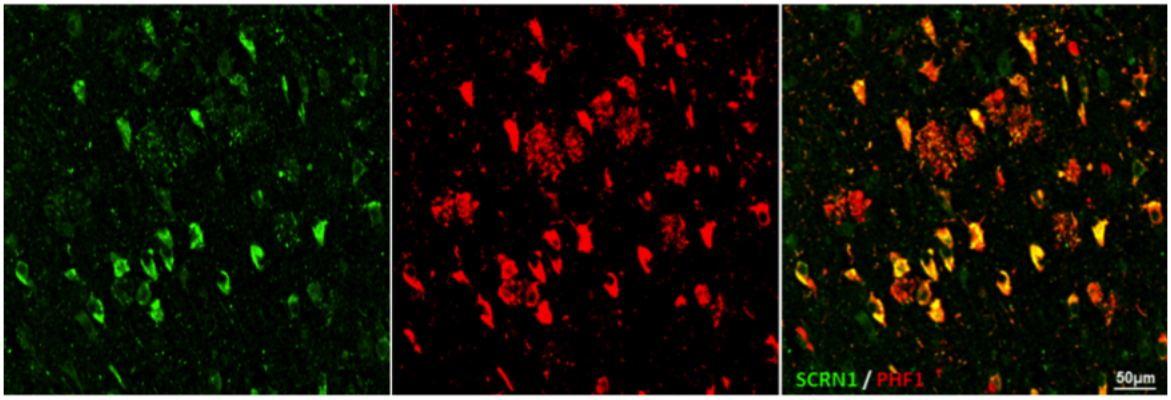

FIGURE 3.4. **SCRN1 in hippocampus of late-stage AD patient**
Representative SCRN1 staining in an AD patient in the hippocampus (images normalized). Note the presence of extracellular PHF1 with little SCRN1 colocalization—these are dystrophic neurites, not NFTs

late-stage AD.

3.3 The expression of SCRN1 is sufficient to classify the pathology of brain tissue

Retraining Inception v3 on images of SCRN1 stained ROIs consistently classified tissue above chance after only 100 iterations. Within and across training sessions, as expected, the validation accuracy (the ability to correctly label the 100 reserved images) would fluctuate. In one training session, the model peaked at 96% accuracy. The model was even able to correctly label ROIs in which there were no NFTs, indicating that SCRN1 expression in AD is distinct even prior to the development of NFTs at a given locus. These results confirm that SCRN1 expression is sufficient to distinguish between AD and NC, even with small ROIs of about 250 neurons.

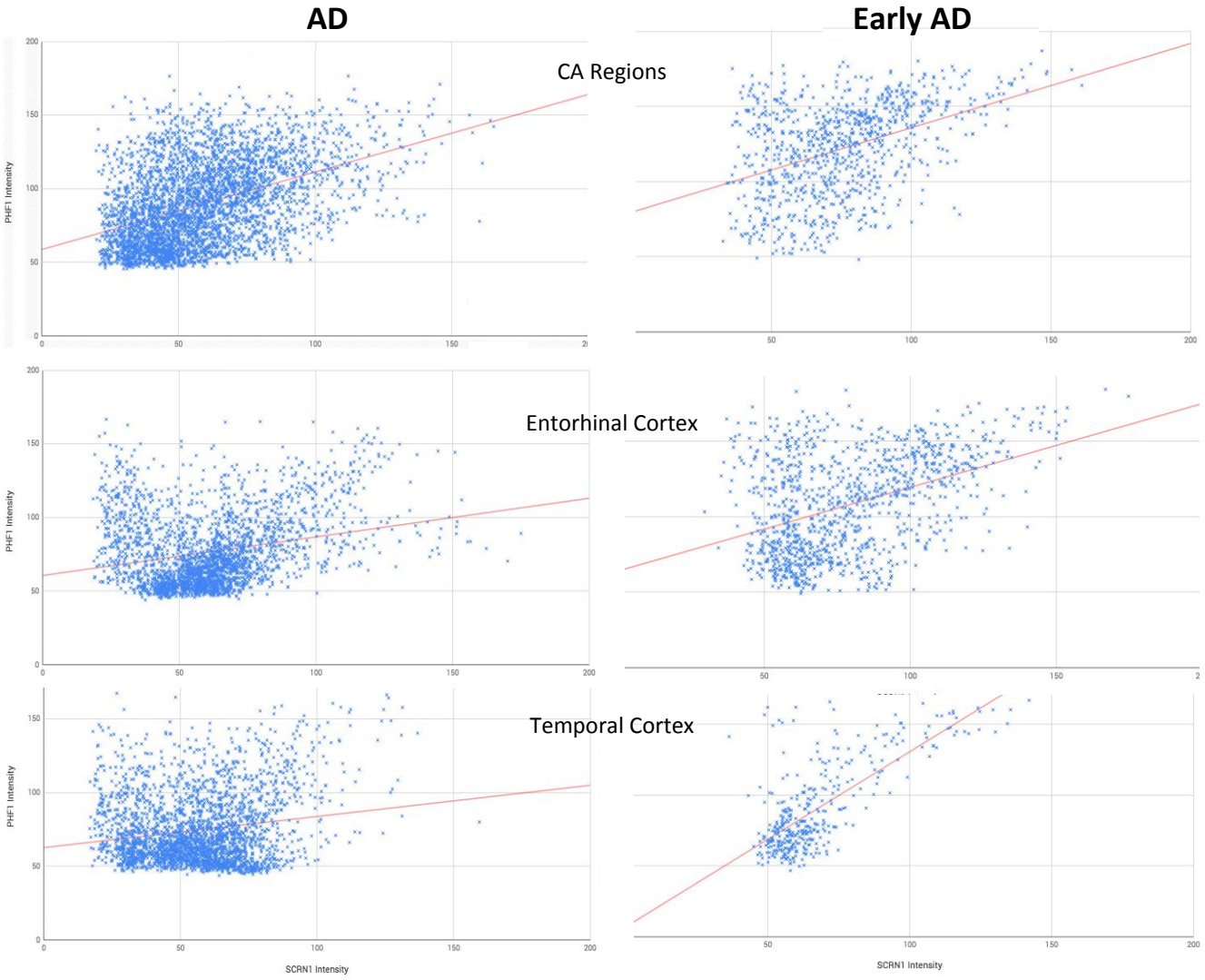

FIGURE 3.5. **The correlation between SCRN1 and PHF1 intensity** Cumulative data from all AD and early AD patients, demonstrating the high correlations between SCRN1 intensity and PHF1 intensity inside of PHF1-positive neurons across the Cornu Ammonis (CA) regions of the hippocampus, ECx, and TCx. (18 AD, 18 early AD). Each point represents an identified object, the horizontal position is determined by the internal pixel intensity of SCRN1, and the vertical position is determined by the internal pixel intensity of PHF1 ($p < .00001$ for all regressions, *Pearson's r* critical value distribution, one-tailed)

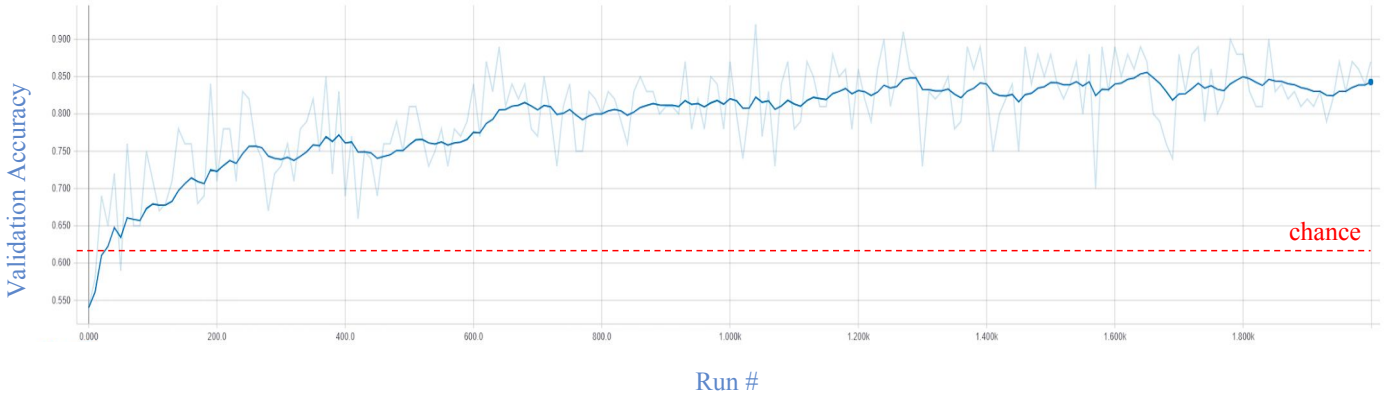

FIGURE 3.6. **Training the classifier**

Validation accuracy as a function of model iteration during a training session. Light blue shows true data, dark blue line represents the data with 90% smoothing. Dashed red line shows the validation accuracy by chance ($p < 0.01$), calculated by the cumulative binomial distribution as proposed by Combrisson et al., 2015

CHAPTER 4

DISCUSSION

This research project is the first to thoroughly characterize an association between SCRN1 and AD, and thus may open doors to drug targets and novel avenues of exploration in AD. I demonstrate here that SCRN1: (i) consistently colocalizes with both established AD hallmarks across regions of the brain and stages of the disease, (ii) is positively correlated with the expression of PHF1 inside of neurons affected by AD, and (iii) has expression patterns that are sufficient to classify the pathology of the patient based on a small tissue sample. The convergence of these findings provides a powerful framework for understanding SCRN1's involvement in AD. Additionally, the questions that arise from this project far outnumber the answers, which is what makes this discovery so fascinating—what features of the SCRN1 protein makes its involvement in AD tractable? Does the manipulation of SCRN1 expression in animal models reduce the pathological or cognitive burdens of AD hallmarks?

The colocalization of SCRN1 and Aβ was among the first discoveries in the lab that hinted at the involvement of SCRN1 in AD. While the trend is not as strong or apparent as I would eventually find it to be with NFTs, SCRN1 unquestionably colocalizes

with plaques in the areas immediately surrounding the hippocampus, and colocalizes to a greater degree in the cortical regions surrounding it. Because of the decades of research that implicate Aβ and AD, this result offers half of the foundation for the first of the aforementioned pillars in my thesis, the second half of which is provided by the colocalization of PHF1 and SCRN1 in the hippocampus, ECx, and TCx in both early onset and late-stage AD brains.

While further studies must be conducted to substantiate it, the positive correlation between SCRN1 and PHF1 intensities foreshadows a co-dependence between SCRN1 and NFTs. Again, the implications of such a dynamic cannot be understated: should NFT development show a dependence on the expression or conformational state of SCRN1, then manipulating such features in SCRN1 could theoretically abolish the accrual of NFTs inside of neurons, and thus remediate or prevent the cognitive debilitation that occurs in AD. SCRN1 expression can be used to predict the expression of PHF1 inside of a given neuron (and vice-versa), and this finding only further strengthens the potential involvement of SCRN1 in the development of AD.

The third and final pillar of this thesis is that the expression of SCRN1 alone is enough to identify a given ROI as from an AD or NC patient. The success of the machine learning model's ability to classify SCRN1-stained ROIs shows that SCRN1 expression in AD is distinct from its typical expression patterns. Because SCRN1 expression patterns in AD are distinct, it opens the door to SCRN1 serving as a biomarker for AD pathology. Whether shifts in SCRN1 expression in the brain have the capacity to predict the development of AD remains unknown; however, the given that early AD data were voided from this particular analysis, it remains unclear.

The results from this thesis serve as direct evidence for the involvement and contributions of SCRN1 to AD pathology. AD is shown here to be involved at all stages of the disease and all studied regions of the brain. Given the devastating and burgeoning

impact of AD, from health care, to society, to families and communities, the need for a cure or symptom-alleviating drug for the disease has never been more timely. While further investigation into the basis of SCRN1's involvement in AD is warranted and imminent, this project proposes a novel protein in AD, and may crack the door to a new chapter of research in AD, with SCRN1 in full focus.

ACKNOWLEDGEMENTS

I would like to take the opportunity to thank my fellow researchers and mentors, who have not only helped shape and build this project, but have also done the same for my career as an undergraduate researcher and burgeoning neuroscientist.

Without question, I would not be here without the guidance and patience of Dr. Eleanor Drummond and Geoffrey Pires. I could not imagine working with a better duo than Eleanor and Geoffrey. In times where I lacked the belief in myself, both Eleanor and Geoffrey, without fail, helped me to regain it. I also want to give a special thanks to Dr. Thomas Wisniewski, whose encouragement to apply to competitive opportunities, as well as his willingness to write letters of recommendation, have led to my awarding of various funding opportunities. I also thank Dr. Wisniewski for offering to take me on in his lab. My experience in the Wisniewski Lab has been one of the most formative experiences in my professional career, and for that, I am eternally grateful.

On the more logistical side, Geoffrey and Eleanor supervised and guided my first experiments with each novel technique, and thus I acknowledge and thank them for their patience while I learned. With the exception of a few instances, Geoffrey and I did all of the stainings used in this thesis, both together and separately. While the proteomic analysis of Aβ plaques was conducted outside the lab, I contributed various samples that were sent in for analysis. Geoffrey took the confocal microscope images of our stained slides in Figures 3.1 and 3.4, which allowed for those beautifully detailed images that enriched this thesis, and I modified his Figures in 2.1 and 2.2. In terms of the analysis, I came up with the idea of conducting the regression analysis and executed it with no supervision. Additionally, I built the machine learning pipeline unsupervised. Finally, I conducted all the computer programming and resulting analyses on my own.

Funding came from 3 Dean's Undergraduate Research Funds, as well as 2 years of support from the National Institutes of Health program, BP-ENDURE. I am grateful to the reviewing bodies for accepting me as a recipient of these competitive awards.

Finally, I would like to acknowledge my family–specifically, Leila, Mom, Bop Bop, NaNa, Uncle Dave, Max, my cousins in Europe, and El Chapo the Dog. Their love and support has enabled my successful pursuit of my passions.

BIBLIOGRAPHY

[1] Ayyadevara S, Balasubramaniam M, Parcon PA, Barger SW, Griffin WST, Alla R, Tackett AJ, Mackintosh SG, Petricoin E, Zhou W, Reis RJS (2016)
Proteins that mediate protein aggregation and cytotoxicity distinguish alzheimer's hippocampus from normal controls.
Aging Cell 15:924–939.

[2] Combrisson E, Jerbi K (2015)
Exceeding chance level by chance: The caveat of theoretical chance levels in brain signal classification and statistical assessment of decoding accuracy.
J Neurosci Methods 250:126–136.

[3] Drummond E, Nayak S, Faustin A, Pires G, Hickman RA, Askenazi M, Cohen M, Haldiman T, Kim C, Han X, Shao Y, Safar JG, Ueberheide B, Wisniewski T (2017)
Proteomic differences in amyloid plaques in rapidly progressive and sporadic alzheimer's disease.
Acta Neuropathologica 133:933–954.

[4] Drummond E, Nayak S, Pires G, Ueberheide B, Wisniewski T (2018)
Isolation of amyloid plaques and neurofibrillary tangles from archived alzheimer's disease tissue using laser-capture microdissection for downstream proteomics.
Methods in Molecular Biology 1723:319–334.

[5] Drummond E, Nayak S, Ueberheide B, Wisniewski T (2015)
Proteomic analysis of neurons microdissected from formalin- fixed, paraffin-embedded alzheimer's disease brain tissue.
Scientific Reports 5:15456.

[6] Ikeda K, Akiyama H, Arai T, Nishimura T (1998)
Glial tau pathology in neurodegenerative diseases: their nature and comparison with neuronal tangles.
Neurobiol Aging 1:S85–91.

[7] Jr LO, Feiner L, Lang E, Szendrei GI, Goedert M, Lee VM (1994)
Monoclonal antibody phf-1 recognizes tau protein phosphorylated at serine residues 396 and 404.
J Neurosci Res. 39:669–673.

[8] Liang-Hao Guo P, Alexopoulos P, Wagenpfeil S, Kurz A, , Perneczky R (2013)
Plasma proteomics for the identification of alzheimer's disease.
Alzheimer Dis Assoc Disord. 4:337–42.

[9] Ping L, Duong DM, Yin L, Gearing M, Lah JJ, Levey AI, Seyfried NT (2018)
Global quantitative analysis of the human brain proteome in alzheimer's and parkinson's disease.
Scientific Data 5.

[10] Selkoe DJ, Hardy J (2016)
The amyloid hypothesis of alzheimer's disease at 25 years.
EMBO Mol Med. 6:595–608.

[11] Szegedy C, Vanhoucke V, Ioffe S, Shlens J (2015)
Rethinking the inception architecture for computer vision.
arxiv .

[12] Wang J, Gu BJ, Masters CL, Wang YJ (2017)
A systemic view of alzheimer disease — insights from amyloid-β metabolism beyond the brain.
Nature Reviews Neurology 13:pages 612–623.

[13] Way G, Morrice N, Smythe C, O'Sullivan AJ (2002)
Purification and identification of secernin, a novel cytosolic protein that regulates exocytosis in mast cells.
Molecular Biology of the Cell 13:2977–3368.